

Inhibition of Melanoma Cell-Intrinsic Tim-3 Stimulates MAPK-Dependent Tumorigenesis



Tobias Schatton^{1,2}, Yuta Itoh¹, Christina Martins¹, Erik Rasbach^{1,3}, Praveen Singh¹, Mariana Silva¹, Kyla Mucciarone⁴, Markus V. Heppt^{1,5}, Jenna Geddes-Sweeney¹, Kate Stewart¹, Anne Brandenburg^{1,6}, Jennifer Liang¹, Charles J. Dimitroff⁷, Martin C. Mihm Jr^{1,†}, Jennifer Landsberg⁶, Christoph Schlapbach⁸, Christine G. Lian⁴, George F. Murphy⁴, Thomas S. Kupper¹, Matthew R. Ramsey¹, and Steven R. Barthel¹

ABSTRACT

T-cell immunoglobulin mucin family member 3 (Tim-3) is an immune checkpoint receptor that dampens effector functions and causes terminal exhaustion of cytotoxic T cells. Tim-3 inhibitors are under investigation in immuno-oncology (IO) trials, because blockade of T-cell-Tim-3 enhances antitumor immunity. Here, we identify an additional role for Tim-3 as a growth-suppressive receptor intrinsic to melanoma cells. Inhibition of melanoma cell-Tim-3 promoted tumor growth in both immunocompetent and immunocompromised mice, while melanoma-specific Tim-3 overexpression attenuated tumorigenesis. Ab-mediated Tim-3 blockade inhibited growth of immunogenic murine melanomas in T-cell-competent hosts, consistent with established antitumor effects of T-cell-Tim-3 inhibition. In contrast, Tim-3 Ab administration stimulated tumorigenesis of both highly and lesser immunogenic murine and human melanomas in T-cell-deficient mice, confirming growth-promoting

effects of melanoma-Tim-3 antagonism. Melanoma-Tim-3 activation suppressed, while its blockade enhanced, phosphorylation of pro-proliferative downstream MAPK signaling mediators. Finally, pharmacologic MAPK inhibition reversed unwanted Tim-3 Ab-mediated tumorigenesis in T-cell-deficient mice and enhanced desired antitumor activity of Tim-3 interference in T-cell-competent hosts. These results identify melanoma-Tim-3 blockade as a mechanism that antagonizes T-cell-Tim-3-directed IO therapeutic efficacy. They further reveal MAPK targeting as a combination strategy for circumventing adverse consequences of unintended melanoma-Tim-3 inhibition.

Significance: Tim-3 is a growth-suppressive receptor intrinsic to melanoma cells, the blockade of which promotes MAPK-dependent tumorigenesis and thus counteracts antitumor activity of T-cell-directed Tim-3 inhibition.

Introduction

Immune checkpoint inhibitors (ICI) have shown unprecedented clinical activity in patients with advanced stage cancers of diverse etiology (1). Nevertheless, clinical benefit is highly variable among patients, highlighting the need for more effective treatment modalities. A promising approach in this regard is to overcome mechanisms of

resistance to ICI therapy (2). For example, induction of other immune checkpoints, such as T-cell immunoglobulin mucin family member 3 (Tim-3), has been associated with resistance to ICI regimens targeting programmed cell death-1 (PD-1; refs. 3, 4). Moreover, Tim-3 inhibition synergizes with PD-1:PD-L1 axis antagonists in preclinical immuno-oncology (IO) models (5–7) and can improve tumor-specific T-cell immunity in some patients with cancer compared with PD-1 blockade alone (8). Together, these findings have generated excitement regarding Tim-3 as a promising IO target (9). Thus, several Tim-3 inhibitors have entered cancer clinical trials, either alone or in combination with PD-1 therapy, for the treatment of hematologic malignancies and solid tumors, including melanoma (8).

Tim-3 is a member of the TIM family of immunoregulatory proteins primarily studied in T cells (9). In cancer, engagement of the Tim-3 receptor by its predominant ligand, Galectin-9, dampens effector functions and causes terminal exhaustion of cytotoxic T cells (10). Consequently, Tim-3 blocking Abs reverse T-cell exhaustion to rein-vigorate antitumor immunity (6, 7). However, preclinical efficacy of Tim-3 monotherapy is modest compared with PD-1 interference (8), raising potential concerns regarding the clinical benefit of Tim-3-based ICI regimens, and especially single-agent Tim-3 blockade, in patients with solid tumors.

Several aspects of Tim-3 immunobiology have been recognized as potential confounders impacting clinical success of Tim-3 checkpoint inhibition (8). For instance, Tim-3 interacts at distinct binding pockets with multiple ligands, including Galectin-9, high-mobility group box 1 (HMGB1), phosphatidylserine (PtdSer), and carcinoembryonic antigen-related cell adhesion molecule 1 (CEACAM-1), with diverse roles in antitumor immunity (9). Accordingly, reported differences in ligand-neutralizing activity of Tim-3 inhibitors (8, 11) could result

¹Harvard Skin Disease Research Center, Department of Dermatology, Brigham and Women's Hospital, Harvard Medical School, Boston, Massachusetts.

²Department of Medicine, Boston Children's Hospital, Harvard Medical School, Boston, Massachusetts. ³Department of Surgery, University Hospital Mannheim, Heidelberg University, Mannheim, Germany. ⁴Department of Pathology, Brigham and Women's Hospital, Harvard Medical School, Boston, Massachusetts.

⁵Department of Dermatology, University Hospital Erlangen, Friedrich-Alexander-University (FAU) Erlangen-Nuremberg, Erlangen, Germany. ⁶Department of Dermatology and Allergology, University Hospital Bonn, Bonn, Germany.

⁷Department of Translational Medicine, Translational Glycobiology Institute at FIU, Herbert Wertheim College of Medicine, Florida International University, Miami, Florida. ⁸Department of Dermatology, University of Bern, Bern, Switzerland.

T. Schatton and Y. Itoh contributed as co-first authors to this article.

[†]Deceased author.

Corresponding Authors: Steven R. Barthel, Department of Dermatology, Brigham and Women's Hospital, Harvard Medical School, 77 Avenue Louis Pasteur, Boston, MA 02115. Phone: 617-525-5698; Fax: 617-525-5571; E-mail: sbarthel@bwh.harvard.edu; and Tobias Schatton, tschatton@bwh.harvard.edu

Cancer Res 2022;82:3774–84

doi: 10.1158/0008-5472.CAN-22-0970

©2022 American Association for Cancer Research

in divergent clinical outcomes. Tim-3 therapeutic efficacy could also depend on the relative frequency of Tim-3-expressing cell types in the tumor microenvironment (TME). Indeed, Tim-3 is not only expressed by T cells, but also by multiple additional immune and nonimmune cell types with varying ligand positivity, resultant Tim-3 receptor signaling and functions (8). For example, in leukemic stem cells (LSC), Tim-3:Galectin-9 interactions promote self-renewal (12). Thus, direct targeting of LSC-Tim-3 is thought to contribute to the observed preliminary efficacy of Tim-3 therapy in patients with leukemia (8). Tim-3 expression by cancer cells has also been reported in solid malignancies (13–15), although little is known about the significance of cancer cell-intrinsic Tim-3 in solid tumor progression and therapy. Because melanoma cells are known to express immune checkpoints (16–19) as well as Tim-3 ligands, including Galectin-9 (20–22), we sought to characterize Tim-3 functional expression by melanoma cells and investigate possible effects of melanoma cell-directed Tim-3 targeting on tumorigenesis.

Here, we report expression of Tim-3 directly on melanoma cells in established murine and human cell lines and patient tumor biospecimens. RNAi-mediated inhibition of melanoma cell-Tim-3 in both immunocompetent and immunocompromised, but not Galectin-9 null mice, significantly increases tumor growth. Conversely, enforced expression of melanoma cell-Tim-3 suppresses tumorigenesis in wild-type, but not Galectin-9-deficient hosts. Tim-3 Ab blockade inhibits growth of immunogenic murine melanomas in T-cell-competent, but promotes tumorigenesis of both highly and lesser immunogenic murine and human melanomas in T-cell-deficient mice. Melanoma cell-Tim-3 activation reduces, while Tim-3 blockade enhances phosphorylation of pro-proliferative Tim-3 signaling mediators (12, 23), including the MAPK effectors, MEK1/2 and ERK1/2. Consistently, pharmacologic MAPK inhibition, using trametinib, reverses unwanted Tim-3 Ab-mediated tumorigenesis in immunocompromised, and enhances desired antitumor effects of Tim-3 inhibition in immunocompetent, hosts. Our results identify Tim-3 as a growth-inhibitory receptor intrinsic to melanoma cells. By stimulating tumorigenesis, inadvertent melanoma-Tim-3 blockade could thus counteract clinical benefit from T-cell-directed Tim-3 therapy. We uncover MAPK inhibition as a combination strategy for circumventing such adverse effects of melanoma cell-Tim-3 interference.

Materials and Methods

Melanoma cell lines, culture methods, and clinical melanoma specimens

Authenticated, *Mycoplasma*-free human and murine melanoma cell lines were obtained from ATCC or Millipore Sigma between 2016 and 2018 and cultured no longer than 3 weeks after thawing, as described in the Supplementary Materials and Methods. Human peripheral blood mononuclear cells (PBMC) were obtained from healthy donors, and clinical tumor biospecimens from patients with melanoma in accordance with protocols approved by the Mass General Brigham Institutional Review Board (IRB), under protocol numbers 2019P001246, 2018P001983, and 2013P001014. Informed consent was obtained from all subjects, and all studies were conducted in accordance with the Declaration of Helsinki. Single-cell suspensions were generated from human melanoma grafts using collagenase digestion, as described previously (17).

RT-PCR, RT-qPCR, and flow cytometry

The full-length coding sequences of human and murine Tim-3 mRNAs (*HAVCR2* and *Havcr2*, respectively) were amplified and

sequenced following reverse transcription of total mRNA using Tim-3 gene-specific primer pairs. The full coding sequences (CDS) of *HAVCR2* (NM_032782.5) expressed by the human A2058 and G361 melanoma cell lines and of *Havcr2* (NM_134250.2) expressed by the murine B16-F10 melanoma cell line were submitted to the GenBank database under the following accession numbers: MW055427 (A2058), MW055428 (G361), and MW055429 (B16-F10). Relative *HAVCR2* and *Havcr2*, or *LGALS9* and *Lgals9* were determined by RT-qPCR and calculated using the $2^{(-\Delta\Delta C_t)}$ method (primers described in the Supplementary Materials and Methods). Tim-3 surface and Galectin-9 protein expression and binding of recombinant soluble murine Galectin-9 (R&D Systems, 3535-GA-050) by established melanoma lines and/or immune cell positive controls were analyzed by flow cytometry, as described previously (17). Tim-3⁺ and Tim-3⁻ melanoma cell subsets were isolated by FACS, following Tim-3 surface staining as above.

Western blot and phosphoprotein array analyses

Cells were lysed, total protein separated by SDS-PAGE and transferred to a polyvinylidene difluoride membrane by electroblotting, as described in detail in the Supplementary Materials and Methods. Expression levels of human and murine Tim-3 and of phosphorylated versus total ERK1/2 or MEK1/2 (Cell Signaling Technology, clones D13.14.4E and 137F5, 41G9 and 61B12, respectively) were determined using enhanced chemiluminescence or the Odyssey CLx imaging system (LI-COR Biosciences). Expression levels of phosphorylated versus respective total protein controls in Tim-3 variant and/or Ab-treated melanoma lines were quantified by the Phospho Explorer Antibody Array (Full Moon Biosystems, PEX100) and/or via densitometric quantification of protein bands using ImageJ (NIH).

Immunofluorescence staining

Immunofluorescence double labeling for Tim-3 and SOX-10, Galectin-9 and SOX-10, or Galectin-9 and CD45 in formalin-fixed, paraffin-embedded tumor biospecimens obtained from patients with melanoma was performed, as described previously (17).

Generation of stable Tim-3 knockdown and Tim-3-overexpressing, or nuclear GFP-labeled melanoma cell line variants

Stable Tim-3 knockdown (KD) melanoma lines were generated, as described in detail in the Supplementary Materials and Methods, using lentiviral transduction particles containing short hairpin RNAs (shRNA) against human *HAVCR2* or murine *Havcr2*, and Tim-3-overexpressing (OE) melanoma lines by infection with viral particles containing the full-length CDS of *HAVCR2* or *Havcr2*. Melanoma lines stably expressing nuclear GFP were generated by fusing a nuclear localization signal with GFP in the MSCV-N-Flag-HA-GFP vector (Addgene, 41034), followed by retroviral infection, puromycin selection, and single-cell sorting of melanoma cells for high GFP expression.

Three-dimensional melanoma culture

Melanoma tumor sphere cultures of native or melanoma-Tim-3 variant lines were maintained, as described previously (17), in standard culture medium, as above, containing 0.5% (w/v) methyl cellulose, in the presence or absence of anti-human (F38-2E2, BioLegend, 345010) or anti-mouse (RMT3-23, BioLegend, 119734) Tim-3 blocking or respective isotype control mAbs.

In vivo tumorigenicity studies

C57BL/6 and NSG mice (17) were purchased from The Jackson Laboratory, and *Lgals9*($-/-$) knockout (KO) C57BL/6 (24) obtained from Dr. Michael Croft (La Jolla Institute for Allergy and Immunology, La Jolla, CA). All mice were female, at least 6 weeks of age, age-matched between experimental groups, maintained and housed at the animal facility of Brigham and Women's Hospital, and used in accordance with the National Institutes of Animal Healthcare Guidelines. All animal experiments were conducted under protocols approved by the Institutional Animal Care and Use Committee of Brigham and Women's Hospital. For tumorigenicity studies, wildtype or *HAVCR2/Havcr2* variant melanoma cells were injected subcutaneously into flanks of recipient mice, as described previously (17, 25). For Tim-3 Ab targeting experiments, melanoma cells were grafted, mice intraperitoneally injected with anti-human (F38-2E2) or anti-mouse (RMT3-23) Tim-3 blocking or isotype control mAbs (200 μ g, respectively) every 3 days starting the day of and/or 15 days after melanoma cell inoculation, and tumor formation and/or growth assessed, as described previously (17). For MEK inhibitor studies, mice were fed a submaximal dose (0.15 mg/kg/day, p.o.) of trametinib (Selleckchem, S2673) or vehicle control (19) incorporated into rodent chow (Research Diets, Inc.).

Statistical analysis

Gene and protein expression levels, tumor spheroid and *in vivo* melanoma growth were compared statistically using the unpaired Student *t* test, the nonparametric Mann-Whitney test (comparison of two experimental groups), one-way ANOVA with Dunnett post-test, repeated-measures two-way ANOVA, or mixed model followed by the Bonferroni correction (comparison of three or more experimental groups). The Spearman rank correlation test was used to measure the degree of association between two variables. Data were tested for normal distribution using the D'Agostino and Pearson omnibus normality test. A two-sided value of $P < 0.05$ was considered statistically significant.

Study approval

All studies involving human specimens were approved by the Mass General Brigham IRB, under protocol numbers 2019P001246, 2018P001983, and 2013P001014. Written informed consent was obtained from all subjects and all studies were conducted in accordance with the Declaration of Helsinki. All animal experiments were conducted under protocols approved by the Institutional Animal Care and Use Committee of Brigham and Women's Hospital.

Data availability

The data generated in this study are publicly available in Genbank under accession numbers MW055427-29 or from the corresponding authors upon reasonable request.

See also the Supplementary Materials and Methods.

Results

Melanomas contain Tim-3-expressing cancer cells

Analysis of a single-cell RNA-sequencing dataset (26) revealed Tim-3 (*HAVCR2*; Fig. 1A) and Galectin-9 (*LGALS9*) mRNA expression by melanoma cells in all patient lesions ($n = 14$) examined, at expression ranges overlapping *HAVCR2* or *LGALS9* levels observed in tumor-infiltrating T cells, B cells, natural killer (NK) cells, macrophages, endothelial cells, and cancer-associated fibroblasts (Supplementary Fig. S1A and S1B). Coexpression of both genes was found in 42.6% of melanoma and 79.4% of T cells (Supplementary Fig. S1C). In The Cancer Genome Atlas PanCancer Atlas (27, 28), *HAVCR2* expression

in melanomas was similar to that in positive control acute myeloid leukemia (AML), while *LGALS9* levels were significantly higher in AML versus melanoma (Supplementary Fig. S2A). *HAVCR2* and *LGALS9* expression levels correlated significantly with each other (Supplementary Fig. S2B) and also tended to correlate inversely with melanoma stage (Supplementary Fig. S2C), but not metastasis (Supplementary Fig. S2D) or overall survival (Supplementary Fig. S2E). Immunofluorescence double labeling of clinical melanoma biospecimens for Tim-3 with the melanocytic lineage marker, SOX-10, confirmed Tim-3 protein expression by up to 10% of SOX-10⁺ melanoma cells in 7 of 15 (Fig. 1B). Galectin-9 was expressed by 12% \pm 3% of SOX-10⁺ cells (mean \pm SEM) and 11% \pm 3% of CD45⁺ lymphocyte positive controls in 11 of 12 patient samples examined (Supplementary Fig. S3A and S3B). Galectin-9 expression tended to be greater in tumors containing Tim-3⁺ cancer cells compared with those without detectable melanoma cell-Tim-3 (Supplementary Fig. S3C). Flow cytometric (FACS) analyses revealed Tim-3 surface and Galectin-9 protein expression by five of five human melanoma cell lines, with greatest surface-Tim-3 positivity (mean \pm SEM) found in A2058 (3.9% \pm 0.5%) and G361 cells (5.0% \pm 0.8%; Fig. 1C), and >85% Galectin-9 positivity across all human lines tested (Supplementary Fig. S3D). Tim-3 surface and Galectin-9 protein expression was also detected in seven of seven murine melanoma lines, with highest Tim-3⁺ cancer cell frequencies observed for B16-F10 (13.5% \pm 0.8%) and YUMMER1.7D4 (15.4% \pm 2.7%) melanoma cells (mean \pm SEM; Fig. 1D) and 42.4%–90.6% Galectin-9 positivity across all murine melanoma lines examined (Supplementary Fig. S3E). RT-PCR amplification and sequencing of the full CDS of the human Tim-3 (*HAVCR2*) and mouse Tim-3 (*Havcr2*) genes revealed Tim-3 mRNA expression by human A2058 and G361 and murine B16-F10 melanoma cells, respectively (Fig. 1E). FACS-based mean fluorescence intensity (Supplementary Fig. S4A) and immunoblot analyses further validated Tim-3 protein expression by human A2058 and G361 and/or murine B16-F10 melanoma cells, at molecular weights corresponding to respective positive controls (Fig. 1F; Supplementary Fig. S4B). RT-qPCR independently confirmed Tim-3 gene expression at varying levels by 13 of 13 human and 8 of 8 murine melanoma lines analyzed (Supplementary Fig. S5A). FACS-purified Tim-3⁺ melanoma cells showed >2- to 21-fold increased *HAVCR2* or *Havcr2* levels compared with Tim-3⁻ A2058, G361, B16-F10, or YUMMER1.7D4 tumor cell subsets, respectively (Supplementary Fig. S5B). Similarly, all human and murine melanoma lines examined showed significant expression (Supplementary Fig. S6A) and enrichment of *LGALS9* and *Lgals9* among Tim-3⁺ versus Tim-3⁻ melanoma subpopulations (Supplementary Fig. S6B). Finally, Tim-3 and Galectin-9 gene coexpression significantly correlated across tumor cell lines (Supplementary Fig. S6C).

Melanoma cell-Tim-3 inhibits murine tumor growth in a Galectin-9-dependent manner

To dissect roles of melanoma cell-Tim-3 in tumorigenesis, we generated stable *Havcr2* KD B16-F10 lines, using two independent shRNAs (Supplementary Fig. S7A), and *Havcr2*-OE B16-F10 melanoma variants (Supplementary Fig. S7B). Compared with respective controls, melanoma-specific *Havcr2*-KD resulted in increased and *Havcr2*-OE in decreased B16-F10 tumor growth in both immunocompetent C57BL/6 (Fig. 2A) and NSG mice lacking adaptive immunity (Fig. 2B). Consistent with our *in vivo* findings, *Havcr2*-KD promoted (Supplementary Fig. S7C), while *Havcr2*-OE impaired *in vitro* three-dimensional B16-F10 culture growth versus controls (Supplementary Fig. S7D). We next examined whether ligation of

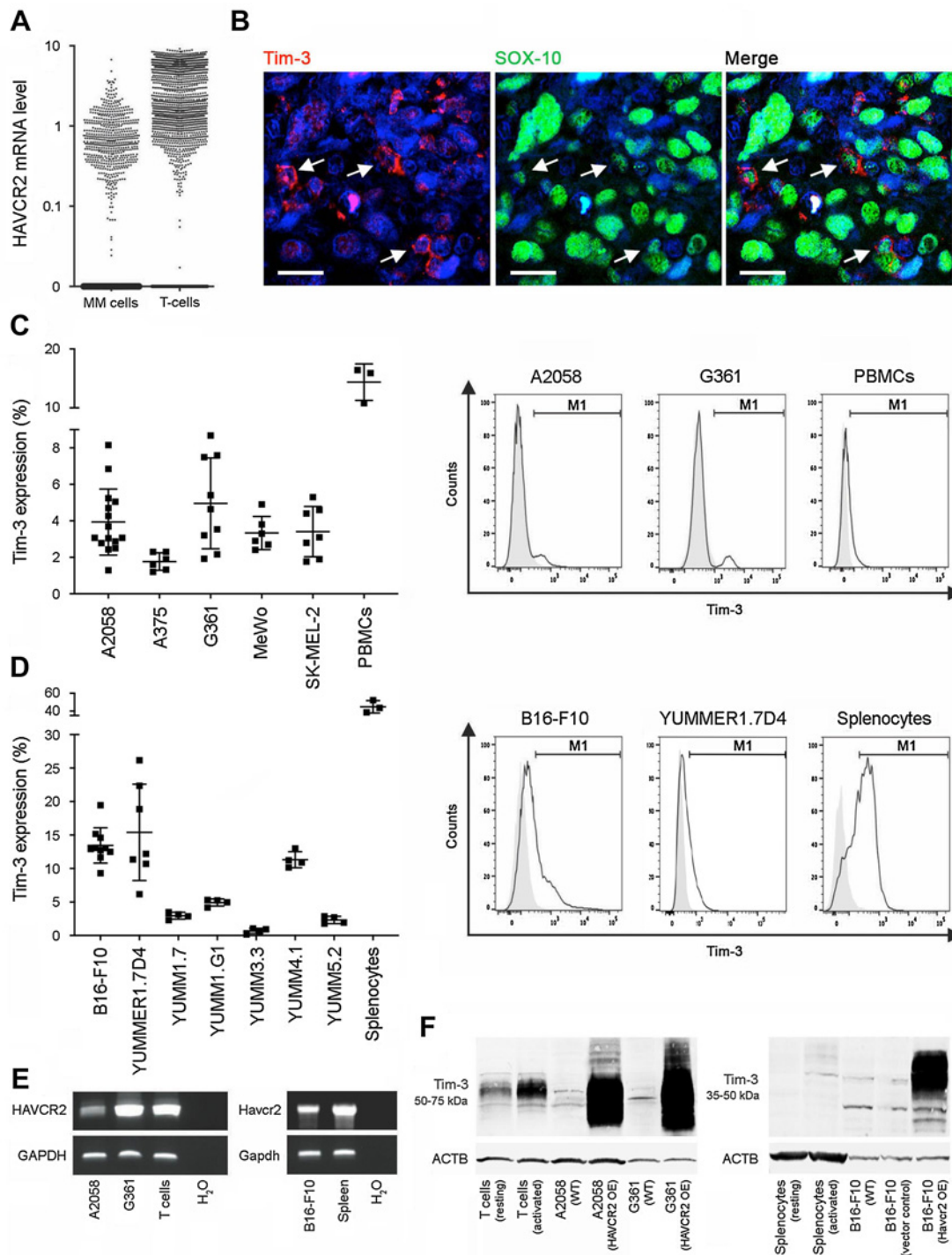


Figure 1.

Tim-3 expression by melanoma cells. **A**, Single-cell RNA-seq analysis of human Tim-3 gene (*HAVCR2*) expression in patient melanoma (MM) cells versus tumor-infiltrating T cells. **B**, Representative dual immunofluorescence staining of a clinical melanoma biopsy for coexpression (arrows) of Tim-3 (red) and the melanocytic marker, SOX-10 (green). Nuclei were counterstained with DAPI (blue). Size bars, 20 μ m. **C** and **D**, Percentages (mean \pm SD; left) and representative flow cytometric histograms (right) of Tim-3 surface protein expression by human melanoma lines and PBMCs (**C**) and by murine melanoma lines and C57BL/6-derived splenocytes ($n = 3$ –10 independent experiments; **D**). **E**, RT-PCR expression analysis of the full-length *HAVCR2* coding sequence by human A2058 and G361 (left) or murine B16-F10 (*Havcr2*; right) melanoma lines and respective T-cell or splenocyte-positive controls. **F**, Immunoblot of Tim-3 protein expression by human (left) or murine (right) wild-type (WT), vector control, and/or Tim-3 (*HAVCR2/Havcr2*)-OE melanoma cells, resting versus activated T-cell or splenocyte-positive controls. See also Supplementary Figs. S1–S6.

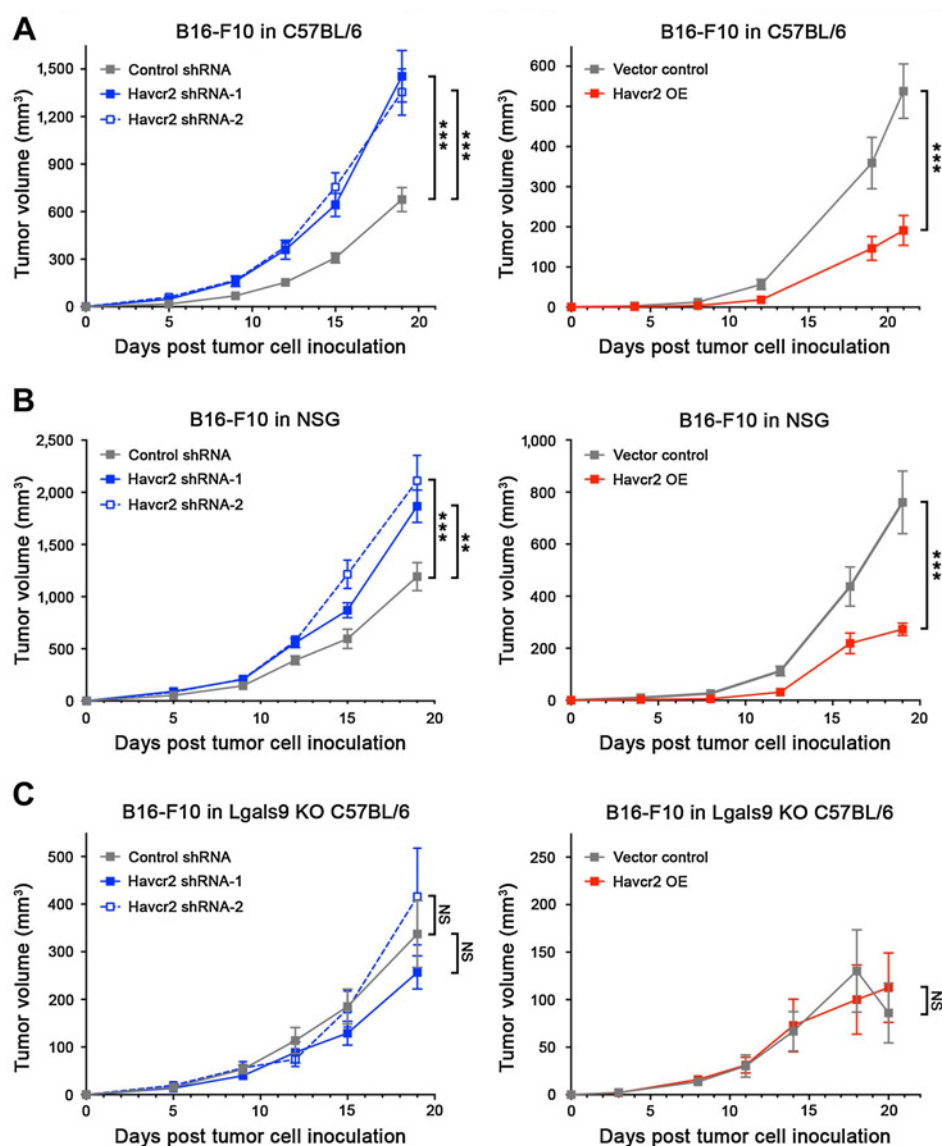


Figure 2. Melanoma cell-Tim-3 inhibits murine tumor growth in a Galectin-9-dependent fashion. Tumor growth kinetics (mean ± SEM) of Tim-3 KD (*Havcr2* shRNA-1/-2; left) and Tim-3-OE (*Havcr2* OE; right) versus shRNA or vector control B16-F10 cells, respectively, in immunocompetent C57BL/6 (A), immunocompromised NSG (B), and Galectin-9 KO (*Lgals9*^{-/-} KO) C57BL/6 mice (C). All experiments were performed in *n* ≥ 10 mice per group on *n* = 2-3 independent occasions. **, *P* < 0.01; ***, *P* < 0.001; NS, not significant. See also Supplementary Fig. S7.

melanoma-Tim-3 to its predominant ligand, Galectin-9, is required for Tim-3-mediated inhibition of tumorigenesis. Compared with vector control cells, *Havcr2*-OE B16-F10 melanoma variants bound significantly higher levels of recombinant Galectin-9 (Supplementary Fig. S7E), confirming Galectin-9 binding by melanoma-expressed Tim-3. The enhancement or suppression of B16-F10 melanoma growth in C57BL/6 (Fig. 2A) or NSG mice (Fig. 2B) resulting from tumor cell-intrinsic *Havcr2*-KD or -OE, respectively, was abrogated in Galectin-9 null (*Lgals9*^{-/-}) C57BL/6 recipients (Fig. 2C), underscoring Galectin-9 involvement in melanoma-Tim-3-dependent regulation of tumorigenesis. These findings uncover melanoma cell-Tim-3-Galectin-9 as a growth-suppressive axis.

Tim-3 Ab blockade inhibits growth of immunogenic murine melanomas in T-cell-competent but promotes tumorigenesis in T-cell-deficient mice

Administration of a Tim-3-blocking Ab known to inhibit Galectin-9 binding (11) did not significantly alter growth of B16-F10 melanomas of poor immunogenicity (25) in T-cell-competent C57BL/6 mice

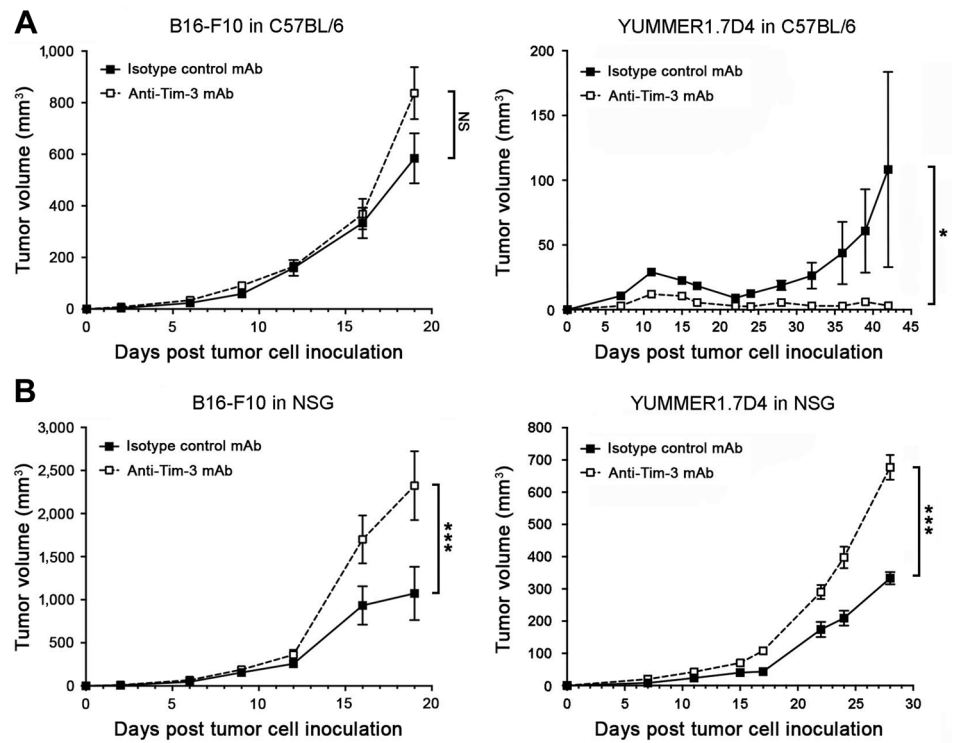
(Fig. 3A), consistent with previous reports (6). In contrast, Tim-3 Ab treatment significantly inhibited growth of highly immunogenic (25) YUMMER1.7D4 tumors in C57BL/6 recipients, compared with controls (Fig. 3A). Conversely, the same Tim-3 blocking Ab promoted growth of three-dimensional *in vitro* tumor cultures (Supplementary Fig. S7F) and tumorigenesis of both B16-F10 and YUMMER1.7D4 melanomas in T-cell-deficient NSG mice (Fig. 3B) expressing high tumoral levels of *Havcr2* and *Lgals9* (Supplementary Fig. S8A and S8B). These results support the possibility that growth stimulation resulting from Ab-based melanoma cell-Tim-3 blockade might antagonize desired antitumor efficacy of T-cell-directed Tim-3 therapy.

Melanoma-Tim-3 inhibits and its blockade promotes human tumor xenograft growth

We next examined the effects of melanoma-specific Tim-3-KD versus Tim-3-OE on human melanoma xenograft growth. Transduction of human A2058 and G361 melanoma cells with two distinct *HAVCR2* shRNAs significantly inhibited (Supplementary Fig. S9A), while infection with *HAVCR2*-OE constructs resulted in marked

Figure 3.

Ab-mediated Tim-3 blockade inhibits growth of immunogenic melanomas in immunocompetent mice but promotes tumorigenesis in T-cell-deficient hosts. Tumor growth kinetics (mean \pm SEM) of B16-F10 (left) or YUMMER1.7D4 (right) wild-type cells in C57BL/6 (A) and NSG mice (B) treated with Tim-3 blocking versus isotype-matched control mAbs. All experiments were performed in $n \geq 10$ mice per group on $n = 2$ independent occasions. *, $P < 0.05$; ***, $P < 0.001$; NS, not significant. See also Supplementary Figs. S7 and S8.

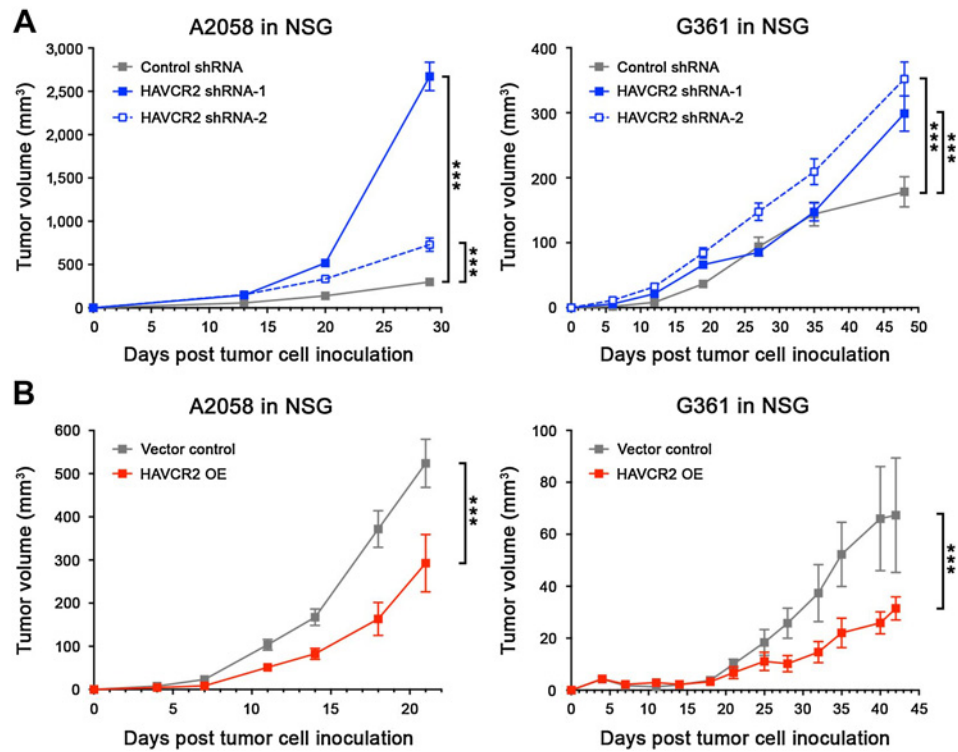


upregulation of both Tim-3 mRNA and protein expression (Supplementary Fig. S9B). Similar to our findings in murine melanoma models (Fig. 2), *HAVCR2*-KD significantly increased (Fig. 4A), while *HAVCR2*-OE decreased human melanoma xenograft growth in NSG mice (Fig. 4B) and three-dimensional culture growth (Supplementary

Fig. S9C and S9D) compared with respective A2058 and G361 controls. Administration of an anti-human Tim-3 blocking Ab known to inhibit Galectin-9 binding (12) significantly increased human tumor xenograft growth in NSG mice (Fig. 5A) and also promoted A2058 and G361 *in vitro* three-dimensional growth (Supplementary Fig. S9E).

Figure 4.

Tim-3 expression by human melanoma cells inhibits tumorigenesis. Tumor growth kinetics (mean \pm SEM) in NSG mice of Tim-3 KD (*HAVCR2* shRNA-1/-2; A) and Tim-3-OE (*HAVCR2* OE; B) versus respective control human A2058 (left) and G361 (right) melanoma cell inoculates ($n = 10$ each, representative of $n = 3$ independent experiments, respectively). ***, $P < 0.001$. See also Supplementary Fig. S9.



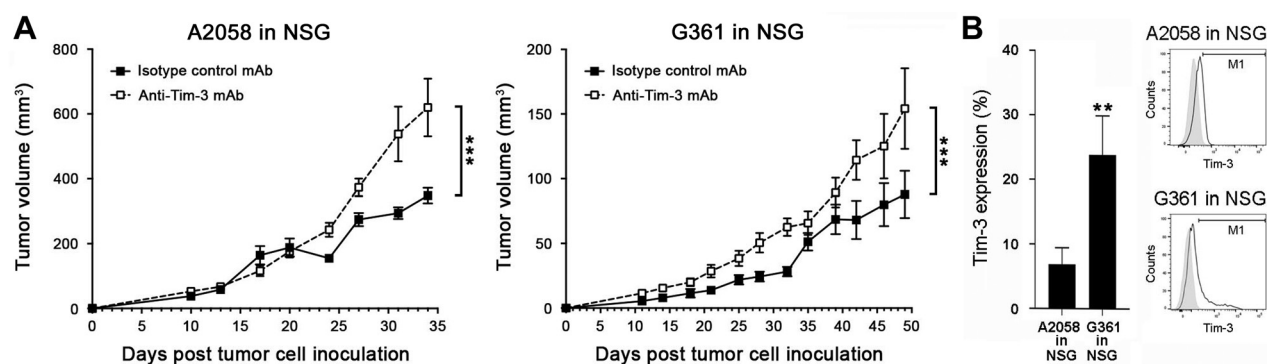


Figure 5.

Ab-mediated human melanoma-Tim-3 blockade promotes tumorigenesis. **A**, Tumor growth kinetics (mean ± SEM) of wild-type A2058 (left) and G361 (right) cells in NSG mice treated with human-specific anti-Tim-3 blocking versus isotype-matched control mAbs ($n = 4-10$ each, representative of $n = 3$ independent experiments). **B**, *In vivo* reactivity (% positive cells, mean ± SEM; left) of the anti-human Tim-3 blocking mAb used in **A** and **B**, with nuclear GFP-labeled A2058 and G361 melanoma cells isolated from tumor xenografts 3 weeks after tumor cell inoculation into NSG mice ($n = 4-6$ each). Representative histogram plots are shown on the right. **, $P < 0.01$; ***, $P < 0.001$. See also Supplementary Fig. S10.

Consistent with the more pronounced growth-promoting effect of this human-specific (Supplementary Fig. S9F) Tim-3 blocking Ab on G361 versus A2058 melanoma xenografts, particularly at early timepoints (<3 weeks; Fig. 5A), binding of the Ab to tumor target cells was significantly higher in G361 ($23.9\% \pm 6.1\%$) compared with A2058 tumors ($6.9\% \pm 2.5\%$) 3 weeks after tumor cell inoculation (mean ± SEM; Fig. 5B). Both *HAVCR2* and *LGALS9* were detected at significant levels in A2058 and G361 tumor xenografts (Supplementary Fig. S10A and S10B). These results further support Tim-3 as a growth suppressor intrinsic to cancer cells, the inhibition of which stimulates tumorigenesis in both murine and human melanomas.

Inhibition of the melanoma-Tim-3 downstream signaling pathway, MAPK, reverses unwanted growth stimulation of melanoma cell-Tim-3 blockade

We next systematically analyzed melanoma cell-intrinsic Tim-3 effector pathways to identify candidate targets for reversal of unwanted protumorigenic effects of melanoma-Tim-3 inhibition. Specifically, we subjected human *HAVCR2*-OE A2058 and G361 and murine *Havcr2*-OE B16-F10 versus respective vector control cells to an unbiased phosphoarray encompassing 1,318 phospho-specific Abs covering more than 30 signaling pathways (29), followed by STRING protein association network analysis. We found three major clusters associated with melanoma-Tim-3 downstream signaling pathway activity, MAPK, NFκB, and cell-cycle regulators (Fig. 6A). The predominant phosphoprotein cluster enriched among *HAVCR2*-OE melanoma cells consisted of pro-proliferative MAPK members with decreased phosphorylation relative to controls, including MEK1 (Fig. 6A), consistent with the observed growth-inhibitory activity of melanoma cell-Tim-3. Immunoblotting confirmed MAPK pathway suppression in *HAVCR2*-OE versus vector control A2058 (top) and G361 (bottom) cells, as evidenced by reduced phosphorylation of the MAPK effector molecules, MEK1/2 and ERK1/2 (Fig. 6B; Supplementary Fig. S11A and S11B). Consistently, shRNA- or Tim-3 blocking Ab-mediated inhibition of melanoma cell-Tim-3 increased MEK1/2 and ERK1/2 phosphorylation compared with respective controls (Fig. 6B; Supplementary Fig. S11A and S11B). We next examined whether MAPK pathway inhibition, using the FDA-approved MEK1/2 inhibitor, trametinib (30), can reverse unwanted growth stimulation of Ab-mediated melanoma-Tim-3 blockade. Accordingly, we treated

NSG mice with a submaximal trametinib dose that significantly inhibits melanoma growth, but does not fully eliminate tumors (19), to enable assessment of Tim-3-dependent, pro-proliferative MAPK effects. This regimen significantly reversed Tim-3 Ab-induced growth of human A2058 and G361 melanoma xenografts (Fig. 6C). We next assessed the effect of combined Tim-3 Ab and MEK inhibition on melanoma growth in immunocompetent hosts. Similar to our findings in human melanoma cells (Fig. 6B), Ab-mediated Tim-3 blockade of YUMMER1.7D4 cells increased MEK1/2 phosphorylation compared with isotype control (Fig. 6D; Supplementary Fig. S11C). Consistently, combined trametinib and Tim-3 Ab administration inhibited YUMMER1.7D4 tumor growth more effectively than either treatment alone in immunocompetent C57BL/6 mice when therapy was initiated the day of or 15 days after tumor cell engraftment (Fig. 6E and F). Combined trametinib and Tim-3 Ab therapy completely eradicated tumors at the experimental endpoint in 7 of 10 and 2 of 10 mice, respectively, but only in 1 of 20 mice receiving Tim-3 monotherapy and none in any other control group (Fig. 6E and F). Together, these results identify MAPK as a melanoma-intrinsic Tim-3 receptor target, which is induced via melanoma cell-Tim-3 blockade to promote tumorigenesis. Consequently, MAPK inhibition counteracts the unwanted growth stimulation from melanoma-Tim-3 antagonism in T-cell null hosts and enhances desired antitumor activity of Tim-3 interference in T-cell-competent mice.

Discussion

Tim-3 is an immune checkpoint receptor that triggers T-effector cell exhaustion to promote tumor immune escape (9). Accordingly, Tim-3 has mainly been studied on tumor-infiltrating T cells (31). Using several independent techniques, our study reveals functional Tim-3 expression directly by cancer cells, and coexpression with Galectin-9, in established murine and human lines and patient melanomas. These findings add another layer of complexity to Tim-3 immunobiology, by recognizing tumor cell-intrinsic, in addition to T-cell immunoregulatory Tim-3:Galectin-9 pathway functions, in the TME of solid malignancies. Similarly, Tim-3 is expressed by both LSCs and normal T cells in hematologic disorders (32). Tim-3:Galectin-9 interactions maintain LSC self-renewal through an autocrine stimulatory loop in preclinical models of myeloproliferative disease (12). As in leukemias,

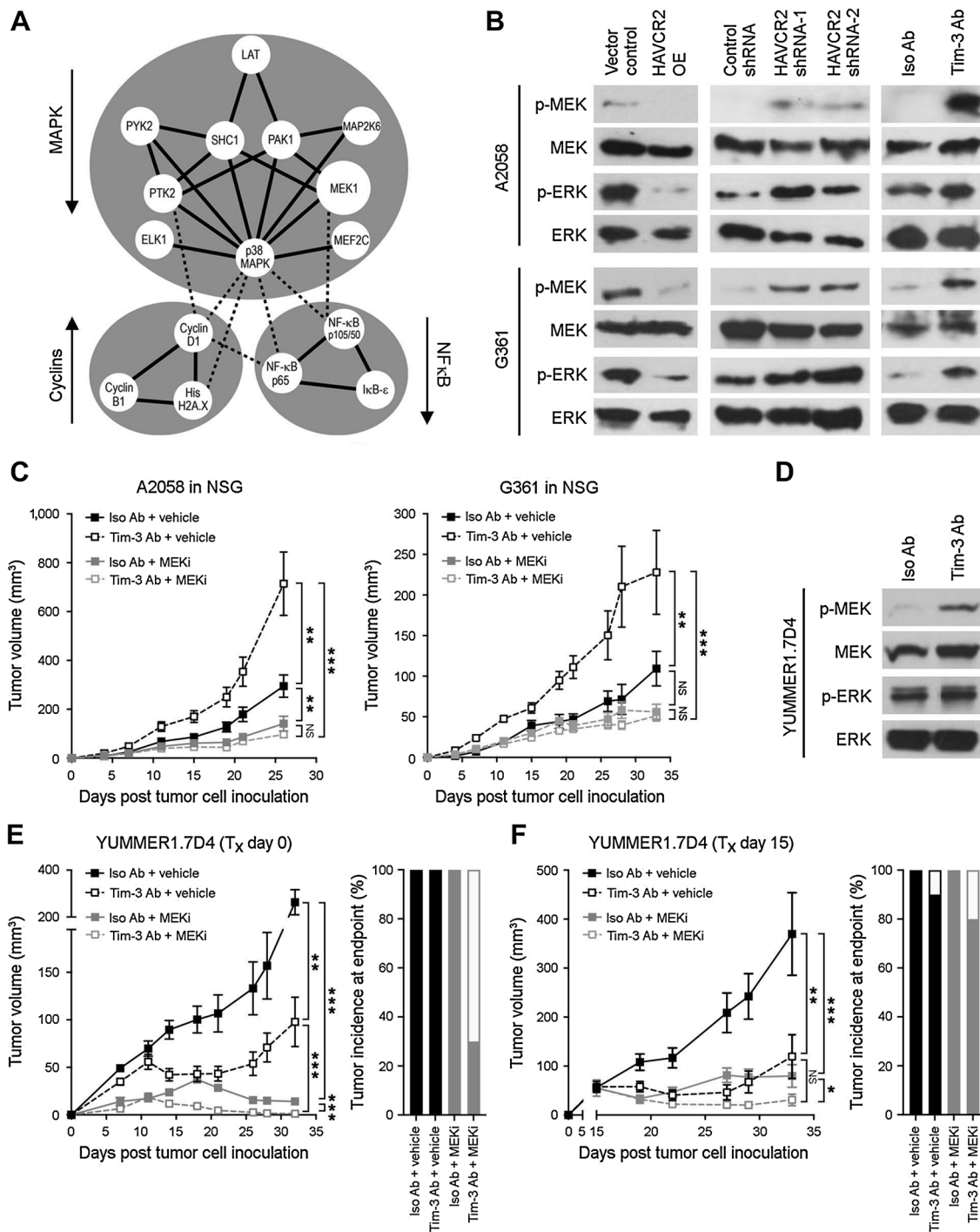


Figure 6.

MEK inhibition reverses melanoma-Tim-3 blockade-mediated growth stimulation. **A**, Protein-protein interaction map (STRING) of differentially phosphorylated proteins (Phospho Explorer Antibody Array) in Tim-3 (*HAVCR2/Havcr2*)-OE versus vector control human A2058 and G361 or murine B16-F10 melanoma cells. Arrows, pathway activation (up) or inhibition (down); solid lines, strong protein-protein interactions; dashed lines, weaker protein-protein interactions. **B**, Immunoblots of phosphorylated (p) and total MEK1/2 and ERK1/2 in vector control versus *HAVCR2* OE (left), control shRNA versus *HAVCR2* KD (shRNA-1/-2; middle), and Tim-3 blocking versus isotype control Ab-treated (right) human A2058 (top) and G361 (bottom) cells. **C**, Tumor growth kinetics (mean \pm SEM) of human A2058 (left) and G361 (right) cells in NSG mice treated with human-specific Tim-3 blocking versus isotype control mAbs, with or without submaximal dosage (0.15 mg/kg/day, orally) of the MEK inhibitor trametinib. **D**, Immunoblots of p- and total MEK1/2 and ERK1/2 in anti-Tim-3 versus isotype control Ab-treated murine YUMMER1.7D4 melanoma cells. **E** and **F**, Tumor growth kinetics (left; mean \pm SEM) and tumor incidence at experimental endpoint (right) of murine YUMMER1.7D4 cells in C57BL/6 mice treated (T_x) with anti-murine Tim-3 blocking versus isotype control mAbs, with or without trametinib (as in **C**) starting on day 0 (**E**) or day 15 (**F**; $n = 10$ mice per treatment group, respectively). *, $P < 0.05$; **, $P < 0.01$; ***, $P < 0.001$; NS, not significant. See also Supplementary Fig. S11.

we found that Tim-3 expression is restricted to subpopulations of melanoma cells, which are nevertheless involved in tumor maintenance. In contrast to LSC-Tim-3, however, the melanoma cell-Tim-3: Galectin-9 axis suppresses tumor growth in multiple models, thus more closely resembling its antiproliferative effects in T cells (9). Moreover, the Tim-3 receptor stimulates downstream NF κ B and MAPK signaling in LSCs (12), while inhibiting said pathways in T cells (8) and melanoma cells, as shown in our study (Fig. 7). Consistently, whereas Tim-3 and Galectin-9 are associated with tumor virulence in leukemias (32), Tim-3, and Galectin-9 expression in melanomas correlate with improved patient survival in some datasets (21), and decreases with tumor stage, as found herein. We are cognizant that these analyses do not discriminate between transcript expression among cell types. Nevertheless, these correlative data are supportive of growth-suppressive Tim-3:Galectin-9 functions in melanoma.

Disease-associated and cell context-dependent differences in Tim-3 receptor signaling and function could result from tissue-associated variations in Tim-3 ligand expression and possibly also immunoregulatory activity. Indeed, Tim-3 interacts with multiple ligands with divergent tissue distribution and roles in cell proliferation and immune homeostasis, including Galectin-9, CEACAM-1, HMGB1, and PtdSer (9). Whether differences in Tim-3 ligand expression, binding, or immunomodulation contribute to opposing Tim-3 signaling between distinct cell types or tissues will require careful dissection in a future dedicated study. Nevertheless, our work involving Galectin-9-deficient mice clearly identifies Galectin-9 as a critical mediator of Tim-3-dependent growth suppression in melanoma cells, like in T cells (9), and in contrast to protumorigenic Galectin-9 effects in leukemic cells (12). Intriguingly, melanoma growth was markedly

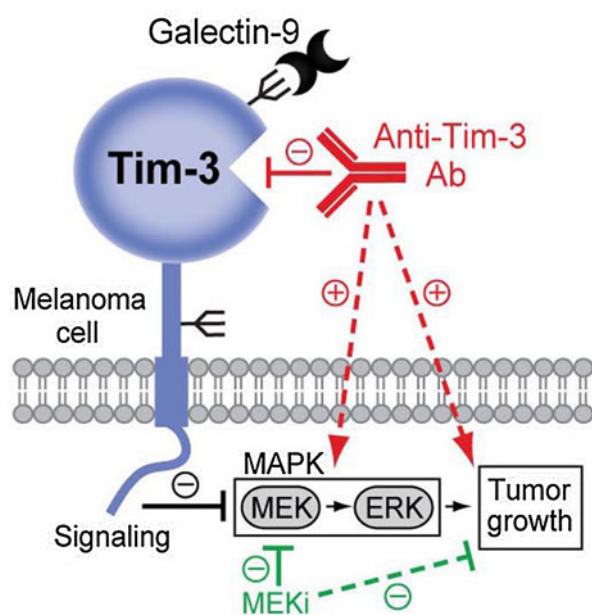


Figure 7.

Therapeutic implications of the melanoma cell-intrinsic-Tim-3 signaling axis. The melanoma cell-Tim-3 receptor binds Galectin-9 and suppresses MAPK signaling to inhibit tumor growth (black, solid line). Ab-based melanoma-Tim-3 blockade (red solid line) activates MAPK effectors, MEK and ERK, thereby unintentionally promoting tumorigenesis (red dashed lines). Combination therapy with MEK inhibitors (MEKi) reverses Tim-3 Ab-mediated MEK activation (green solid line), leading to desirable melanoma growth suppression (green, dashed line).

suppressed in Galectin-9 KO versus wildtype mice, but stimulated via melanoma-Tim-3 inhibition, thus implying additional Galectin-9 roles in tumorigenesis independent of melanoma-Tim-3. Indeed, Galectin-9 interacts with multiple alternative receptors, some of which have known protumorigenic functions, including PD-1 (22).

Several ICIs targeting Tim-3 have entered clinical IO trials for melanoma and other cancers (8). Therefore, our findings that melanoma-Tim-3 interference stimulates tumorigenesis are concerning, because inadvertent blockade of the melanoma cell-Tim-3:Galectin-9 axis in patients could antagonize desired efficacy of T-cell-directed Tim-3 therapy. One might thus predict that clinical-grade Tim-3 inhibitors with low affinity for melanoma cell-Tim-3 would elicit greater clinical benefit than those with high melanoma-Tim-3 binding. Because unwanted blockade of melanoma-Tim-3 by clinical inhibitors might pose an obstacle to successful T-cell-Tim-3 therapy, we believe that consideration in trial design and interpretation is warranted. It should be noted that therapeutic outcomes might not merely depend on relative Tim-3 Ab affinity for T cells versus melanoma cells, but also on melanoma immunogenicity or reactivity with other Tim-3-expressing TME cell types, including dendritic cells (33), myeloid (14), and natural killer cells (34). Moreover, while inhibition of cancer cell-Tim-3 promotes tumor growth in some malignancies, as reported herein, it suppresses tumorigenesis in other cancers, such as leukemias (12), to synergize with T-cell-Tim-3 blockade. Tim-3 therapeutic efficacy could thus vary between tumor entities based on disease-specific variations in cancer cell-intrinsic or TME cell-Tim-3 pathway functions.

In scenarios where inadvertent antagonism of cancer cell-intrinsic Tim-3 stimulates growth, concurrent targeting of protumorigenic Tim-3 downstream pathways could improve outcomes. Indeed, we found that pharmacologic inhibition of the melanoma-Tim-3 signaling effector, MEK1/2, reverses unwanted tumorigenesis caused by melanoma-Tim-3 blockade. Because MEK inhibitors, including trametinib, have been approved by the FDA for the treatment of melanomas harboring BRAF-activating mutations (30), they should be considered for Tim-3-based combination therapy in patients. In support, combined Tim-3 Ab and trametinib administration inhibited both tumor initiation and growth of established immunogenic YUM-MER1.7D4 melanomas in immunocompetent hosts to a greater extent than either therapy alone. In addition to thwarting tumor-intrinsic oncogenic signaling, MEK inhibitors synergistically promote T-cell immunity when combined with ICI regimens (35) including Tim-3 inhibitors (31), further underscoring the promise of dual Tim-3-MEK inhibitor modalities. In melanomas lacking BRAF mutations, targeting of other Tim-3 signaling mediators (12, 23), such as NF κ B, might provide an alternative strategy for reversing unwanted consequences of tumor cell-Tim-3 blockade.

In summary, we identify an additional role for Tim-3 as a growth-inhibitory receptor intrinsic to melanoma cells. Because melanoma-Tim-3 blockade stimulates MAPK-dependent tumorigenesis, it could antagonize benefit from T-cell-directed Tim-3 therapy. This provides a therapeutic rationale for implementing Tim-3 Abs with greater T-cell selectivity or combining Tim-3 with MAPK pathway inhibitors (Fig. 7). Such cell type-directed Tim-3 targeting strategies could help overcome unintended protumorigenic effects of melanoma-Tim-3 interference and maximize desired anticancer T-cell activity.

Authors' Disclosures

T. Schatton reports grants from NIH/NCI, V Cancer Foundation, and Harvard Stem Cell Institute during the conduct of the study. E. Rasbach reports grants from German Research Foundation (DFG) during the conduct of the study. C. Schlapbach reports grants from Peter Hans Hofschneider Professorship for Molecular Medicine,

Swiss National Science Foundation, Bern Center for Precision Medicine, and Ruth & Arthur Scherbarth Foundation during the conduct of the study; personal fees from Abbvie, LEO Pharma, Lilly, and Novartis, PPM Services outside the submitted work. G.F. Murphy reports grants from Brigham and Women's Hospital during the conduct of the study. S.R. Barthel reports grants from NIH/NCI, V Cancer Foundation, Harvard Stem Cell Institute, Melanoma Research Alliance, Outrun the Sun, and Brigham Research Institute during the conduct of the study. No disclosures were reported by the other authors.

Authors' Contributions

T. Schatton: Conceptualization, resources, data curation, formal analysis, supervision, funding acquisition, validation, investigation, visualization, methodology, writing—original draft, project administration, writing—review and editing. **Y. Itoh:** Data curation, formal analysis, validation, investigation, visualization, methodology. **C. Martins:** Data curation, formal analysis, validation, investigation, visualization, methodology. **E. Rasbach:** Data curation, formal analysis, validation, investigation. **P. Singh:** Data curation, formal analysis, validation, investigation, methodology. **M. Silva:** Data curation, formal analysis, validation, investigation, visualization, methodology. **K. Mucciarone:** Data curation, formal analysis, validation, investigation. **M.V. Heppt:** Investigation. **J. Geddes-Sweeney:** Data curation, formal analysis, investigation. **K. Stewart:** Data curation, formal analysis, investigation. **A. Brandenburg:** Data curation, formal analysis, investigation. **J. Liang:** Formal analysis, investigation. **C.J. Dimitroff:** Resources. **M.C. Mihm:** Resources, supervision, project administration. **J. Landsberg:** Resources. **C. Schlapbach:** Resources, investigation. **C.G. Lian:** Resources, data curation, investigation. **G.F. Murphy:** Resources, investigation. **T.S. Kupper:** Resources, project administration. **M.R. Ramsey:** Resources. **S.R. Barthel:** Conceptualization, resources, data curation, formal analysis, supervision, funding acquisition, validation, investigation, visualization, methodology, writing—original draft, project administration, writing—review and editing.

References

- Sharma P, Allison JP. Immune checkpoint targeting in cancer therapy: toward combination strategies with curative potential. *Cell* 2015;161:205–14.
- Kalbasi A, Ribas A. Tumour-intrinsic resistance to immune checkpoint blockade. *Nat Rev Immunol* 2020;20:25–39.
- Koyama S, Akbay EA, Li YY, Herter-Sprie GS, Buczkowski KA, Richards WG, et al. Adaptive resistance to therapeutic PD-1 blockade is associated with upregulation of alternative immune checkpoints. *Nat Commun* 2016;7:10501.
- Shayan G, Srivastava R, Li J, Schmitt N, Kane LP, Ferris RL. Adaptive resistance to anti-PD1 therapy by Tim-3 upregulation is mediated by the PI3K-Akt pathway in head and neck cancer. *Oncoimmunology* 2017;6:e1261779.
- Fourcade J, Sun Z, Benallaoua M, Guillaume P, Luescher IF, Sander C, et al. Upregulation of Tim-3 and PD-1 expression is associated with tumor antigen-specific CD8+ T cell dysfunction in melanoma patients. *J Exp Med* 2010;207:2175–86.
- Ngiow SF, von Scheidt B, Akiba H, Yagita H, Teng MW, Smyth MJ. Anti-TIM3 antibody promotes T cell IFN-gamma-mediated antitumor immunity and suppresses established tumors. *Cancer Res* 2011;71:3540–51.
- Sakuishi K, Apetoh L, Sullivan JM, Blazar BR, Kuchroo VK, Anderson AC. Targeting Tim-3 and PD-1 pathways to reverse T cell exhaustion and restore anti-tumor immunity. *J Exp Med* 2010;207:2187–94.
- Acharya N, Sabatos-Peyton C, Anderson AC. Tim-3 finds its place in the cancer immunotherapy landscape. *J Immunother Cancer* 2020;8:e000911.
- Wolf Y, Anderson AC, Kuchroo VK. TIM3 comes of age as an inhibitory receptor. *Nat Rev Immunol* 2020;20:173–85.
- Das M, Zhu C, Kuchroo VK. Tim-3 and its role in regulating anti-tumor immunity. *Immunol Rev* 2017;276:97–111.
- Sabatos-Peyton CA, Nevin J, Brock A, Venable JD, Tan DJ, Kassam N, et al. Blockade of Tim-3 binding to phosphatidylserine and CEACAM1 is a shared feature of anti-Tim-3 antibodies that have functional efficacy. *Oncoimmunology* 2018;7:e1385690.
- Kikushige Y, Miyamoto T, Yuda J, Jabbarzadeh-Tabrizi S, Shima T, Takayanagi S, et al. A TIM-3/Gal-9 autocrine stimulatory loop drives self-renewal of human myeloid leukemia stem cells and leukemic progression. *Cell Stem Cell* 2015;17:341–52.
- Cao Y, Zhou X, Huang X, Li Q, Gao L, Jiang L, et al. Tim-3 expression in cervical cancer promotes tumor metastasis. *PLoS One* 2013;8:e53834.
- Komohara Y, Morita T, Annan DA, Horlad H, Ohnishi K, Yamada S, et al. The coordinated actions of TIM-3 on cancer and myeloid cells in the regulation of tumorigenicity and clinical prognosis in clear cell renal cell carcinomas. *Cancer Immunol Res* 2015;3:999–1007.
- Zhuang X, Zhang X, Xia X, Zhang C, Liang X, Gao L, et al. Ectopic expression of TIM-3 in lung cancers: a potential independent prognostic factor for patients with NSCLC. *Am J Clin Pathol* 2012;137:978–85.
- Clark CA, Gupta H, Sareddy GR, Pandeswara S, Lao S, Yuan B, et al. Tumor-intrinsic PD-L1 signals regulate cell growth, pathogenesis and autophagy in ovarian cancer and melanoma. *Cancer Res* 2016;76:6964–74.
- Kleffel S, Posch C, Barthel SR, Mueller H, Schlapbach C, Guenova E, et al. Melanoma cell-intrinsic PD-1 receptor functions promote tumor growth. *Cell* 2015;162:1242–56.
- Mo X, Zhang H, Preston S, Martin K, Zhou B, Vadalia N, et al. Interferon-gamma signaling in melanocytes and melanoma cells regulates expression of CTLA-4. *Cancer Res* 2018;78:436–50.
- Sanlorenzo M, Vujic I, Floris A, Novelli M, Gammaitoni L, Giraudo L, et al. BRAF and MEK inhibitors increase PD-1-positive melanoma cells leading to a potential lymphocyte-independent synergism with anti-PD-1 antibody. *Clin Cancer Res* 2018;24:3377–85.
- Wiersma VR, de Bruyn M, van Ginkel RJ, Sigar E, Hirashima M, Niki T, et al. The glycan-binding protein galectin-9 has direct apoptotic activity toward melanoma cells. *J Invest Dermatol* 2012;132:2302–5.
- Holderried TAW, de Vos L, Bawden EG, Vogt TJ, Dietrich J, Zarbl R, et al. Molecular and immune correlates of TIM-3 (HAVCR2) and galectin 9 (LGALS9) mRNA expression and DNA methylation in melanoma. *Clin Epigenetics* 2019;11:161.
- Yang R, Sun L, Li CF, Wang YH, Yao J, Li H, et al. Galectin-9 interacts with PD-1 and TIM-3 to regulate T cell death and is a target for cancer immunotherapy. *Nat Commun* 2021;12:832.
- Lee J, Su EW, Zhu C, Hainline S, Phuah J, Moroco JA, et al. Phosphotyrosine-dependent coupling of Tim-3 to T-cell receptor signaling pathways. *Mol Cell Biol* 2011;31:3963–74.
- Seki M, Oomizu S, Sakata KM, Sakata A, Arikawa T, Watanabe K, et al. Galectin-9 suppresses the generation of Th17, promotes the induction of regulatory

Acknowledgments

The authors thank Dr. Michael Croft (La Jolla Institute for Allergy and Immunology, La Jolla, CA) for providing Galectin-9-deficient mice for our study.

This work was supported by a Merck-Melanoma Research Alliance Young Investigator Award, a V Foundation for Cancer Research Scholar Grant, an Outrun the Sun Melanoma Research Scholar Award, a Fund to Sustain Research Excellence from the Brigham Research Institute, Brigham and Women's Hospital (to S.R. Barthel), a Developmental Project Grant from the Harvard Stem Cell Institute, and NIH/NCI grants R01CA247957, R01CA258637 (to S.R. Barthel and T. Schatton), and R01CA190838 (to T. Schatton). Partial support was provided by a Mizutani Foundation for Glycoscience Research Grant, NIH/NCI grant U01CA225644, and NIH/NIAID grant R21AI146368 (to C.J. Dimitroff), a Walter Benjamin Fellowship from the German Research Foundation (DFG; to E. Rasbach), a Martin Mihm Fellowship from the German Society of Dermatopathology (ADH; to M.V. Heppt), and a DFG Scholarship (to A. Brandenburg) as part of Germany's ImmunoSensation² Excellence Initiative (EXC 2151).

The publication costs of this article were defrayed in part by the payment of publication fees. Therefore, and solely to indicate this fact, this article is hereby marked "advertisement" in accordance with 18 USC section 1734.

Note

Supplementary data for this article are available at Cancer Research Online (<http://cancerres.aacrjournals.org/>).

Received March 24, 2022; revised July 14, 2022; accepted August 11, 2022; published first August 18, 2022.

- T cells, and regulates experimental autoimmune arthritis. *Clin Immunol* 2008; 127:78–88.
25. Wang J, Perry CJ, Meeth K, Thakral D, Damsky W, Micevic G, et al. UV-induced somatic mutations elicit a functional T cell response in the YUMMER1.7 mouse melanoma model. *Pigment Cell Melanoma Res* 2017;30:428–35.
 26. Tirosh I, Izar B, Prakadan SM, Wadsworth MH 2nd, Treacy D, Trombetta JJ, et al. Dissecting the multicellular ecosystem of metastatic melanoma by single-cell RNA-seq. *Science* 2016;352:189–96.
 27. Cerami E, Gao J, Dogrusoz U, Gross BE, Sumer SO, Aksoy BA, et al. The cBio cancer genomics portal: an open platform for exploring multidimensional cancer genomics data. *Cancer Discov* 2012;2:401–4.
 28. Liu J, Lichtenberg T, Hoadley KA, Poisson LM, Lazar AJ, Cherniack AD, et al. An integrated TCGA pan-cancer clinical data resource to drive high-quality survival outcome analytics. *Cell* 2018;173:400–16.
 29. Nold-Petry CA, Lo CY, Rudloff I, Elgass KD, Li S, Gantier MP, et al. IL-37 requires the receptors IL-18Ralpha and IL-1R8 (SIGIRR) to carry out its multifaceted anti-inflammatory program upon innate signal transduction. *Nat Immunol* 2015;16:354–65.
 30. Flaherty KT, Hodi FS, Fisher DE. From genes to drugs: targeted strategies for melanoma. *Nat Rev Cancer* 2012;12:349–61.
 31. Liu Y, Cai P, Wang N, Zhang Q, Chen F, Shi L, et al. Combined blockade of Tim-3 and MEK inhibitor enhances the efficacy against melanoma. *Biochem Biophys Res Commun* 2017;484:378–84.
 32. Jan M, Chao MP, Cha AC, Alizadeh AA, Gentles AJ, Weissman IL, et al. Prospective separation of normal and leukemic stem cells based on differential expression of TIM3, a human acute myeloid leukemia stem cell marker. *Proc Natl Acad Sci U S A* 2011;108:5009–14.
 33. de Mingo Pulido A, Gardner A, Hiebler S, Soliman H, Rugo HS, Krummel MF, et al. TIM-3 regulates CD103(+) dendritic cell function and response to chemotherapy in breast cancer. *Cancer Cell* 2018;33:60–74.
 34. da Silva IP, Gallois A, Jimenez-Baranda S, Khan S, Anderson AC, Kuchroo VK, et al. Reversal of NK-cell exhaustion in advanced melanoma by Tim-3 blockade. *Cancer Immunol Res* 2014;2:410–22.
 35. Ebert PJR, Cheung J, Yang Y, McNamara E, Hong R, Moskalenko M, et al. MAP kinase inhibition promotes T cell and anti-tumor activity in combination with PD-L1 checkpoint blockade. *Immunity* 2016;44:609–21.